Molecular Crystals and Liquid Crystals

Publication details, including instructions for authors and subscription information:
http://www.tandfonline.com/loi/gmcl20

Coarse-Grained Molecular Dynamic Simulations for Lyotropic Liquid-Crystalline Solutions of Semiflexible Rod-Like Molecules

Shaoliang Lin [a], Naoko Numasawa [b], Takuhei Nose [c] & Jiaping Lin [a]

[a] Key Laboratory for Ultrafine Materials of Ministry of Education, School of Materials Science and Engineering, East China University of Science and Technology, Shanghai, China

[b] School of Dentistry, Nihon University, Tokyo, Japan

[c] Department of Nanochemistry, Tokyo Polytechnic University, Atsugi, Kanagawa, Japan

Version of record first published: 22 Sep 2010

To cite this article: Shaoliang Lin, Naoko Numasawa, Takuhei Nose & Jiaping Lin (2007): Coarse-Grained Molecular Dynamic Simulations for Lyotropic Liquid-Crystalline Solutions of Semiflexible Rod-Like Molecules, Molecular Crystals and Liquid Crystals, 466:1, 53-76

To link to this article: http://dx.doi.org/10.1080/15421400701246309

Mol. Cryst. Liq. Cryst., Vol. 466, pp. 53–76, 2007

ISSN: 1542-1406 print/1563-5287 online
DOI: 10.1080/15421400701246309

Coarse-Grained Molecular Dynamic Simulations for Lyotropic Liquid-Crystalline Solutions of Semiflexible Rod-Like Molecules

Shaoliang Lin
Key Laboratory for Ultrafine Materials of Ministry of Education, School of Materials Science and Engineering, East China University of Science and Technology, Shanghai, China

Naoko Numasawa
School of Dentistry, Nihon University, Tokyo, Japan

Takuhei Nose
Department of Nanochemistry, Tokyo Polytechnic University, Atsugi, Kanagawa, Japan

Jiaping Lin
Key Laboratory for Ultrafine Materials of Ministry of Education, School of Materials Science and Engineering, East China University of Science and Technology, Shanghai, China

Coarse-grained molecular dynamic simulations are performed for lyotropic liquid-crystalline (LC) solutions of semiflexible rod-like molecules, which are realized by harmonic-stretching potential and angle-bending potential. The phase behavior and molecular dynamic information are investigated. When the concentration of rod-like molecules increases, the solution transits from isotropic to binary phase and then to anisotropic phase. The influences of chain length, temperature, solvent solubility, and chain rigidity are studied. The simulation for the phase behavior successfully reproduces the predictions of Flory lattice theory on the rod-like molecule solution. The decrement of the chain rigidity increases the concentration of phase transition, and the apparent persistence length is increases by molecular alignments with LC formations at higher concentrations.

Keywords: lyotropic liquid crystal; molecular dynamic simulation; persistence length; phase behavior; rod-like molecule

Address correspondence to Shaoliang Lin, Key Laboratory for Ultrafine Materials of Ministry of Education, School of Materials Science and Engineering, East China University of Science and Technology, Shanghai 200237, China. E-mail: linshaoliang@hotmail.com

INTRODUCTION

Liquid-crystalline phases formed by rod-like molecules have been extensively studied both theoretically [1–3] and experimentally [4–10] because of the unique combinations of solid and liquid properties in liquid crystals (LC). In the theoretical evaluation [2], in a solution of rod-like particle above a critical concentration (threshold volume fraction) depending on the molecule-axis ratio, a transformation from an isotropic to an anisotropic phase is predicted, and the two phases coexist in a discrete range of concentration. Such predictions of lattice theory have qualitatively been confirmed by experimental observations. Experiments on liquid crystallinity exhibited by solutions of α-helical polypeptides have been especially illuminating [4–7]. The qualitative agreement between observed and calculated values of the threshold volume fraction is quite satisfactory. The comparisons of theory and experiments for the other LC polymer systems are also performed by Aharoni [8] and Ciferri et al. [9,10].

Another approach to the studies of LC transitions in polymers is computational simulations. Molecular simulation methods have played an important role in investigating material property studies since the pioneering studies [11–13]. To investigate the phase behavior of an LC system, several different models are employed by a single anisotropic mesogene [14–17] or semiflexible molecules consisting of many particles [18–25]. For a single anisotropic mesogene model, Frenkel et al. carried out molecular dynamic (MD) calculations and constant-pressure Monte Carlo (MC) simulations for hard rods, which are realized by hard parallel spherocylinders consisting of a cylindrical segment of length L and diameter D capped at each end with a hemisphere of the same diameter [14]. Hard spherocylinders with both translational and orientational freedom can form a thermodynamically stable smectic phase. Dense systems of prolate and oblate ellipsoids on the base of an affine transformation model have been studied by Allen et al. [15]. They concluded that the isotropic–nematic transition is greatly weakened by a modest degree of molecular biaxiality. For the semiflexible molecules consisting of many particles, Dijkstra et al. used MC simulation to study the system of semiflexible polymers consisting of hard spherocylinders connected by joints of variable flexibility. The influence of molecular flexibility on the location of the isotropic–nematic phase transition was studied, and they observed a good qualitative agreement with theoretical predictions and experimental results [18]. Zarembo et al. composed semiflexible molecule of soft spheres connected by Frenkel's elastic springs. They found that persistence-length dependences of the jump of order

parameter and boundary volume fractions in isotropic and nematic phases at LC transition agree well with theoretical predictions [24]. All of these simulations are performed for the bulk LC system. However, little attention has been paid to lyotropic LC solutions in this approach. It is well known that incorporating a solvent may greatly affect the phase behavior of LC systems.

MD simulation has received much attention in a sense that comparison with theories and experiments is straightforward. In this work, such a simulation method is applied for a lyotropic LC solution of semiflexible rod-like molecules. We present another candidate of coarse-grained, rod-like molecules consisting of connected atoms, which is realized by harmonic-stretching potential and angle-bending potential. Such a model can provide the rigidity into the chain from sufficient flexibility to high rigidity by changing the bond-angle potential. The phase behavior of the lyotropic LC solution is investigated in terms of the order parameter. The MD information is discussed. The influence of concentration, temperature, and molecular parameters, such as chain length and chain rigidity, are also studied. Some simulation results will be compared with predictions of existing theories.

METHOD OF SIMULATION

The simulations for lyotropic LC solutions are performed using the simulator, the coarse-grained molecular dynamics program (COGNAC) of OCTA. The simulator was developed by Doi's group, which is on a public website [26]. COGNAC aims at covering a large class of molecular models, ranging from full atomistic models to bead-spring models. Such molecular modeling is realized by a combination of choices of various potential functions between chemically bonded pairs and chemically nonbonded pairs.

In this article, the quantities of length, energy, and mass are used in the reduced unit system given in Table 1. The reduced quantities of temperature, time, density, and pressure are obtained as also shown in Table 1. The simulation results presented here are not related to any particular rod-like molecule systems.

Molecular Model of Rod-Like Molecules and the System

The simulation model is designed to represent solutions of solvent and rod-like molecules with various concentrations. Potentials that should be given are bonding potential, U_{mol}, and nonbonding potential, U_{ij}. That is, the potentials that act on the particles (atoms) consist of

TABLE 1 Conversion of the Reduced Unit System

Reduced unit	Value
Reduced length	$1\ \sigma = 0.4\,\text{nm}$
Reduced energy	$1\ \varepsilon = 0.5\,\text{kJ/mol}$
Reduced mass	$1\ \text{m} = 23.3 \times 10^{-27}\,\text{kg}$
Reduced temperature	$1\ T = \varepsilon/R = 60.1\,\text{K}$
Reduced time	$1\ t = \sqrt{A_v m\sigma^2/\varepsilon} = 2.12\,\text{ps}$
Reduced density	$1\ \rho = m/\sigma^3 = 0.363\,\text{g/cm}^3$
Reduced pressure	$1\ P = \varepsilon/(A_v\sigma^3) = 13.0\,\text{MPa}$

R is the gas constant and A_v is the Avogadro's number.

two parts. The former can construct a desired molecule from atoms, whereas the latter describes intermolecular interactions.

A coarse-grained, rod-like molecule is modeled by connecting several beads (or atoms) together with the harmonic springs. To realize the rod-like molecules, the equilibrium angle θ_0 the (angle defined here is the external angle of the common bond angle) is set to be substantially zero, so that no torsional potential is necessarily specified. Bond-stretching potential and angle-bending potential are combined to keep the rigidity of the molecule. Therefore, U_{mol} is expressed by a combination of $U_{bond}\,(r)$ and $U_{angle}\,(\theta)$. The bond-stretching potential is a function of distance, r, between the chemically bonded atoms. A harmonic type is applied and defined by

$$U_{bond}(r) = \frac{1}{2}k_b(r - r_0)^2, \tag{1}$$

where k_b is the bond spring constant and r_0 is the equilibrium bond length.

The following equation is the angle-bending potential, which is a cosine harmonic function of the angle θ defined by the three chemically bonded atoms:

$$U_{angle}(\theta) = \frac{1}{2}k_a(\cos\theta - \cos\theta_0)^2, \tag{2}$$

where k_a is the angle spring constant and θ_0 is the equilibrium angle. The larger the value of k_a, the more rigidity of molecule chain.

To realize the rod-like molecules, the equilibrium angle θ_0 is set as a value of 0.1, and r_0 is 0.75 with $k_b = 10{,}000$. These parameters are fixed for all the simulation calculations. The spring constant k_a is changeable to indicate the rigidity of molecular chain and is set to be 10,000 in most calculations. The mass of a constituting atom is

TABLE 2 Interaction Parameters for LJ Potential

Interaction	r_{ij}^c	σ_{ij}	ε_{ij}
Rod–rod	2.5	1.0	0.5
Rod–solvent	2.5	0.88	0.8, 1.5
Solvent–solvent	2.5	0.75	0.5

set to be 1.8. The solvent molecule consists of a single atom, of which mass is set to be 1.0.

The nonbonding potential U_{ij} is given by the standard Lennard–Jones (LJ) 12:6 potential acting between any two pair of beads i and j:

$$U_{ij} = 4\varepsilon_{ij}\left[\left(\frac{\sigma_{ij}}{r_{ij}}\right)^{12} - \left(\frac{\sigma_{ij}}{r_{ij}}\right)^{6} - \left(\frac{\sigma_{ij}}{r_{ij}^c}\right)^{12} + \left(\frac{\sigma_{ij}}{r_{ij}^c}\right)^{6}\right], \qquad r \le r_{ij}^c, \tag{3}$$

where r_{ij}^c is the cutoff distance beyond which the LJ interaction is set to be 0, $r_{ij} = |r_i - r_j|$ and r_i and r_j are the locations of the ith and jth beads, respectively. In this article, the cutoff distance is kept to 2.5 for any pairs of species. The pairwise interaction ε_{rs} between the atoms of rod-like molecules and solvent is chosen to be variable, whereas the other interactions are set to be 0.5 (i.e., $\varepsilon_{rr} = \varepsilon_{ss} = 0.5$), where subscripts r and s denote rod-like molecule and solvent, respectively. The sets of different values of ε_{rs} lead to the different solubility of the solvent. Hereafter, ε_{rs} is set to be 0.8 in most cases. The choices of the LJ parameters are summarized in Table 2. Atomic masses and the orders of ε and σ used here were selected such that them density and the cohesive energy density in condensed state fall in the ranges of those of ordinary liquids.

Simulation Conditions

All the simulations are carried out on a cubic cell using a dynamic algorithm with temperature–pressure controlling method (NPT ensemble). The pressure and temperature are controlled by the loose-coupling method, whereas the density of the system is allowed to fluctuate throughout the simulation. The loose-coupling method had been described in detail in Ref. 27. Periodic boundary conditions were imposed to minimize the effect of finite system size. A random mode was applied to generate the initial structures of molecules, where solvents and rod-like molecules are randomly distributed in the system and the structure relaxation was done by dynamic simulation. The integration time step $\Delta t = 0.01$ was selected. The length of

simulation runs were 2×10^6 time steps (i.e., 20,000 time units). All calculations were performed at a pressure $P = 20.0$ and temperature $T = 3.0$ without further specification. The number of rod-like molecules in a cell was fixed at 50, and the number of solvent molecules was changed to vary the concentration.

Order Parameter and Orientation Direction

In this simulation, a quantitative measure for the degree of alignment of rod-like molecules is denoted by order parameter S. The order parameter S_i for the single rod-like molecule coded as i can be defined by

$$S_i = \frac{3(u_i \cdot u_d)^2 - 1}{2} \tag{4}$$

where u_i is the normalized vector of ith rod-like molecule and u_d is the normalized vector of orientation direction (the director), which is determined by iteration to find the maximum value of $\overline{S}$ by taking into account the up–down symmetry of the rod-like molecule. Here, the order parameter $\overline{S}$ of the lyotropic LC solution at the kth simulation step is calculated to be the average value of S_i for all rod-like molecules.

For the MD simulation, the thermodynamic systems undergo continual local fluctuations [28]. The order parameter is also fluctuated during the simulation process. The order parameter S of the system at equilibrium can be written by

$$S = \frac{1}{N_s} \sum_{k=1}^{N_s} \overline{S}_k = \langle \overline{S} \rangle, \tag{5}$$

where N_s is the number of collected data of $\overline{S}$ at equilibrium condition. The fluctuation σ_S of order parameter can be written by

$$\sigma_s^2 = \frac{1}{N_s} \sum (S - \overline{S})^2. \tag{6}$$

Chain Rigidity and Persistence Length

The chain rigidity intrinsic to a molecular structure is specified primarily by the spring constant k_a for bond angle, as well as bond length, r_0. The chain rigidity is usually characterized by the correlation $\langle b_i\, b_j \rangle$ between unit bond vectors, b_i and b_j of ith and jth bonds. The correlation is expressed as a function $|i - j|$ as

$$\langle b_i \cdot b_j \rangle = r_0^2 \exp\left(-\frac{r_0 |i - j|}{L_p} \right), \tag{7}$$

where L_p is the persistence length, which is ordinarily used as a parameter of chain rigidity. The persistence is usually considered to be intrinsic to the molecular structure, but actually depends on environment such as solvent and the condensed state. In the present case, the persistence length defined by Eq. (7) may change by chain alignments because of LC formation with changing concentration. Therefore, this nonintrinsic persistence length L_p is here referred to as apparent persistence length, and the persistent length in the isotropic phase, which must be intrinsic to molecular structure, is called persistence length as usual and denoted as l_{p}. In this article, we define some other parameters to describe the apparent rigidity as follows:

We define the rigidity per molecule, which is referred to as apparent molecular rigidity, R_m, and the inverse is referred to as apparent molecular flexibility, F_m. It is given by the following equation:

$$F_m = \frac{1}{R_m} = \frac{L}{L_p}, \tag{8}$$

where L is the rod length given by $r_0\,(N-1)$ with N being the number of atoms in a rod-like molecule.

Volume Fraction

In this article, the concentration of rod-like molecules in the system is identified by volume fraction. The calculation of volume fraction is specified as the following. First plot the equilibrium density of the system as a function of weight fraction of rod-like molecules (shown in Fig. 1), then extrapolate the fitting line to the two extreme cases as the weight fraction equals to 0 and 1.0. The densities of the pure solvent and bulk rod-like molecules in the system can be obtained from the intercept as the value of 1.5181 and 2.4224, respectively. As the densities are known, the volume fraction of rod-like molecules can be calculated for the finite numbers of rod-like and solvent molecules.

RESULTS AND DISCUSSION

In the present calculations, the spring constant k_a set in most cases is 10,000, which corresponds to the persistence length $l_p \approx 50$ in dilute solution. The rod-like molecules studied here have the number of atoms ranging from 8 to 20, corresponding to molecule length from 5.25 to 14.25, so that the molecular lengths are much shorter than l_p; that is, the molecules may be reasonably rigid.

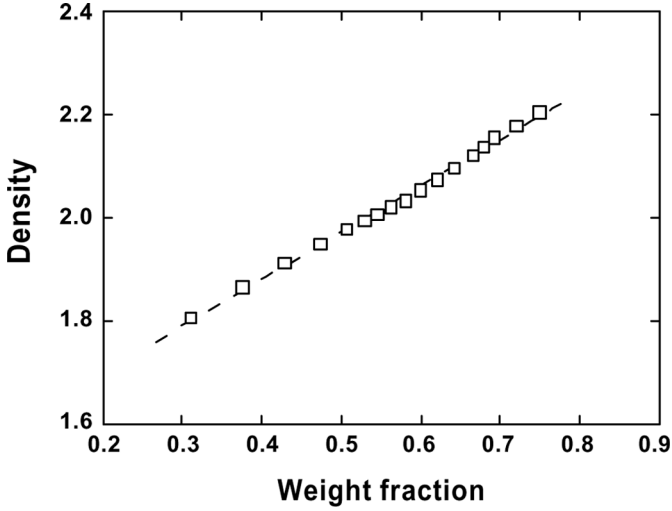

FIGURE 1 Equilibrium density of the system against the weight fraction of rod-like molecules; the fitting function is shown as a dashed straight line.

Time Dependence of Order Parameter

Figure 2 shows two typical results of order parameter $\overline{S}$ as a function of simulation steps. The volume fractions of rod-like molecules are 0.693 and 0.361 for plot (a) and plot (b), respectively. As can be seen from plot (a), the $\overline{S}$ value increased dramatically to a higher value within 5×10^5 simulation steps, and then tends to level off, suggesting the system reaches an equilibrium condition during the simulation process. At the lower volume fraction shown as plot (b), the $\overline{S}$ value fluctuates at a low level, which indicates the system is also at equilibrium. In the present simulation, calculations are performed upto 2×10^6 steps. All quantities of order parameter are averaged over the last 1×10^6 steps. For example, the S values at the equilibrium condition thus obtained for plot (a) and plot (b) are 0.976 and 0.136, respectively.

Concentration Dependencies of the Order Parameter and the Order–Disorder Transition

It is informative to analyze the status of rod-like molecule chains in the solution. To visualize the structures, snapshot pictures of solutions at different volume fractions with rod-like molecule chain length $L = 6.75$ are shown in Fig. 3. Figure 3a shows a typical status of the

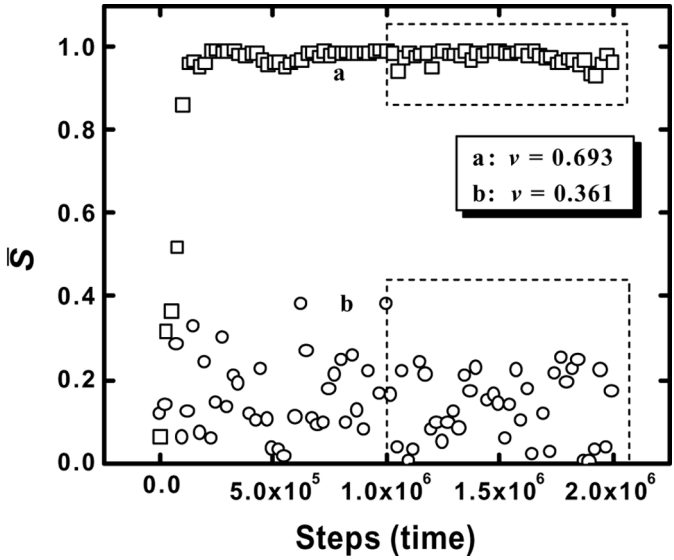

FIGURE 2 Typical results of order parameter $\overline{S}$ as a function of simulation steps at volume fractions of 0.693 (a) and 0.361 (b).

solution in a high volume fraction with a value of 0.653. All of rod-like molecule axes tend to align to one direction. Such a phenomenon indicates the solution is in an anisotropic phase. They exhibit an orientationally ordered nematic phase. When the volume fraction is decreased to 0.506, as observed in Fig. 3b, some rod-like molecules tend to align

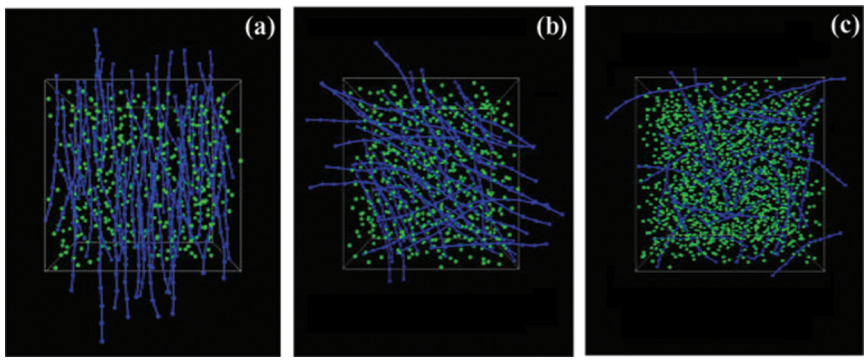

FIGURE 3 Snapshot pictures of lyotropic liquid-crystalline solution at different volume fractions: (a) $v = 0.653$, (b) $v = 0.506$, and (c) $v = 0.273$.

together to form bundles, but they have different directions. Such a solution still shows some order as a whole and may correspond to the binary phase (coexisting of anisotropic and isotropic phase). Unfortunately, the system size used did not allow us to distinguish unambiguously the phase separation of binary phase. Shown in Fig. 3c is a snapshot picture of solution at a low volume fraction of 0.273. In this case, the rod-like molecular orientations are distributed randomly. It shows that the solution is in an isotropic phase. As observed from Fig. 3, the alignment of the rod-like molecules is changed with concentration, which suggests phase transition occurs with decreasing volume fraction.

Meanwhile, by comparing Fig. 3a with Fig. 3c, one can see that in the anisotropic phase, the rod -like molecule chain shows larger apparent persistence length than that in the isotropic phase, because of chain alignments at the high concentration. In the isotropic phase shown in Fig. 3c, some bent rod-like molecules are found, which suggests the chain has more apparent flexibility. The detailed information of apparent chain rigidity is presented later.

Figure 4 shows the normalized vector u_d of orientation axis (the unit vector of director) as a function of simulation time. Three cases, in which volume fractions are the same as those of Fig. 3, are presented for seeing vector fluctuations, where x-, y-, and z-component values of the orientation vector are plotted in each figure. It is noted that the rod-like molecules are set to be randomly distributed in the initial structure of the solution. Figure 4a shows a typical result of vector fluctuations for the anisotropoic phase. With increasing simulation time, the values of x, y, and z tend to level off after 1×10^6 simulation steps. It indicates that the rod-like molecules align in one direction, with the stable ordered phase formed. Shown in Fig. 4b is the orientation vector of the binary phase. A fluctuating but stabilized vector is found during the simulation. As seen in Fig. 4c, the vector in the isotropic phase randomly fluctuates similar to that in the binary phase, but more frequently. The difference in frequency reflects that the molecules in the isotropic dilute solution fluctuate independently in their directions, while some of the molecules make orientational motions with forming a cluster of molecular alignments in the binary phase.

Figure 5 presents the order parameter S of rod-like molecules with chain length of 6.75 as a function of rod- like molecule volume fraction. The S value slightly increases to a value of point (a) at lower concentrations and then increases dramatically to a higher value point (b) and tends to level off at a value closed to 1.0 with increasing the volume fraction. Such a change of S in a sigmoid manner indicates that

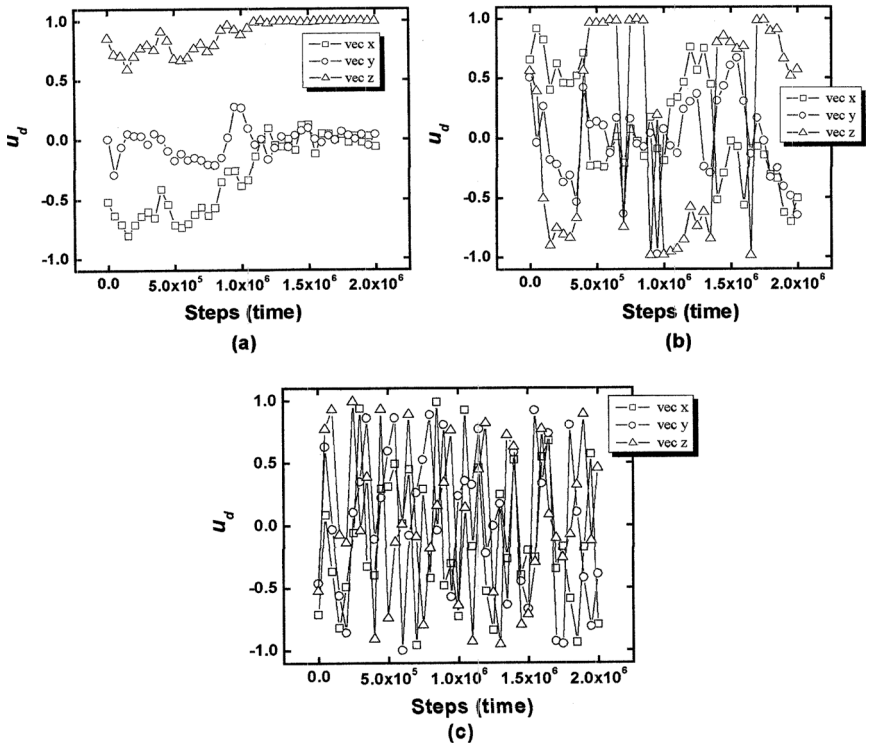

FIGURE 4 Typical results of time dependence (fluctuations) of orientational vector for different volume fractions: (a) $v = 0.653$, (b) $v = 0.506$, and (c) $v = 0.273$.

the phase transition occurs with increasing the rod-like molecule concentration. The inflexions of (a) and (b) shown in Fig. 5 divide the concentration dependence into three different regions. When the volume fraction is larger than (b) point, the rod-like molecule solution shows a high order, which indicates it forms an anistropic (LC) phase. The solution is in an isotropic phase when the volume fraction is less than (a) point, where rod-like molecules are distributed almost randomly as the S value is quite low. When the volume fraction is between (a) point and (b) point, the solution could be of a coexistence of isotropic and anisotropic phases, which is again defined as the binary phase. The critical points (a) and (b) are regarded as phase-transition points from the isotropic phase to the binary phase (IB) and from the binary phase to the anisotropic phase (BA), respectively.

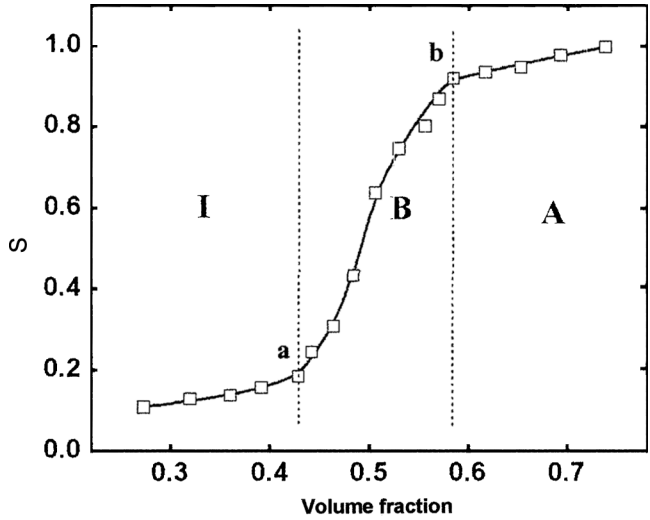

FIGURE 5 Order parameter S as a function of the Volume fraction of rod-like molecules for a chain length L of 6.75: I, isotropic phase, B, binary phase, and A, anisotropic phase.

As is mentioned previously, because of the MD equilibrium, the order parameter value fluctuates both at the higher concentration and lower concentration shown in Fig. 2. The fluctuation value σ_S of order parameter is plotted as a function of rod-like molecule concentration in Fig. 6. The σ_S value increases slightly with increasing the concentration to a critical point (a). The curve of σ_S rises sharply from the critical point (a). It passes through the maximum point (c) with a value about 0.145, then falls rapidly toward another critical point (b) with further increase in concentration, and finally it tends to decrease to zero. Such a change of σ_S with concentration also suggests phase transition occurs. These two critical points can be regarded as phase-transition points. The amount of anisotropic phase may grow at the expense of the isotropic one when the concentration increases from (c) point to (b) point as shown in Fig. 6.

Dependencies of Phase-Transition Concentration on Rod-Like Molecule Chain Length

The influence of rod-like molecule chain length on the phase-transition concentrations is illustrated in Fig. 7, where volume fractions at IB and BA transitions are plotted against the chain length.

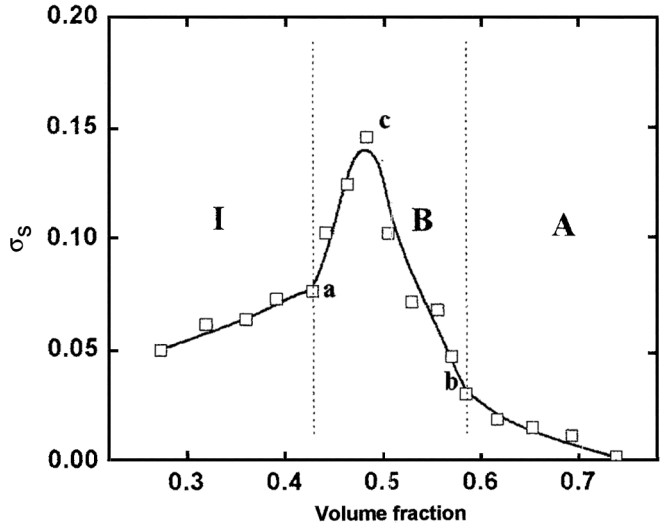

FIGURE 6 Fluctuation value σ_s of order parameter as a function of the Volume fraction of rod-like molecules for chain length L of 6.75: I, isotropic phase; B, binary phase; and A, anisotropic phase.

It is clearly seen that the phase-transition concentrations of both IB and BA shift to lower values as the chain length is increased. Concomitantly with the decreasing of the phase-transition concentrations, the boundary of binary phase is widened.

It is interesting to compare the simulation results with existing theories. Flory lattice model is one of the most popular theories to study the lyotropic LC solution. It has been widely proved by experiments. A typical phase diagram based on Flory lattice model is reploted in the inset plot in Fig. 7. It shows concentration of phases in equilibrium in relation to axis ratio (chain length), x, in solution of rod-like particles, where v_2 and v_2' are phase-transition concentrations of IB and BA in volume fraction, respectively [2]. With increase in x, the concentrations of both phase transitions diminish. Such an influence of chain length based on the lattice model is in line with our simulation result illustrated in Fig. 7. Meanwhile the width of binary phase is first increased and then decreased with increasing x as shown in the inset plot. The present simulation covers the shorter range of chain length and shows widening of the binary phase boundary with increasing chain length, consistent with the theoretical prediction.

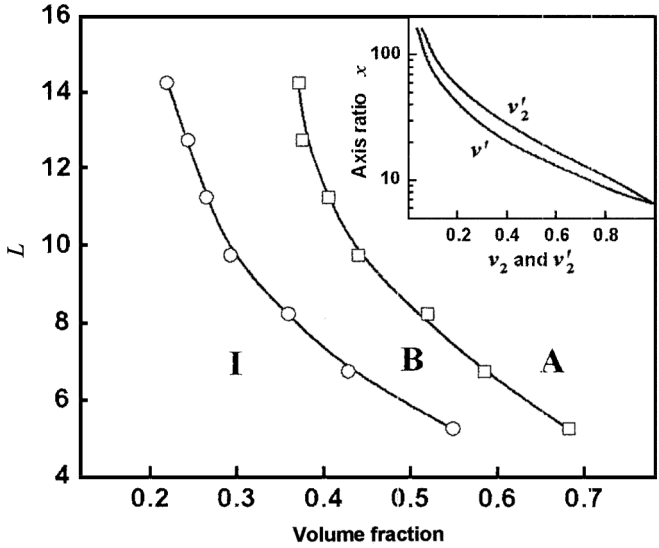

FIGURE 7 Concentration dependence of phase transition as a function of chain length L: I, isotropic phase; B, binary phase; and A, anisotropic phase. The inset plot shows the influence of chain length on phase-transition concentrations based on the Flory lattice model.

Effects of Temperature and Solvent Solubility

Two typical results for the different temperature *(T)* are shown in Fig. 8 with the value of 3.0 (plot a) and 3.5 (plot b). With increasing T, the S curve moves to the higher concentration, suggesting both IB and BA phase-transition concentrations are increased. Simultaneously the boundary of binary phase is widened at the higher temperature.

In Fig. 9 the influence of interaction parameter ε_{rs} between rod-like molecule and solvent is illustrated. The higher value of the ε_{rs} means that the solvent is better for the rod-like molecule. Two cases are shown for the interaction with the ε_{rs} values of 0.8 and 1.5. The influence of solvent quality on the transition behavior is weak. It is seen, however, that the IB phase transition tends to occur at a higher concentration and the BA phase transition tends to occur at a lower one when the ε_{rs} is increased. Concomitantly the boundary of the binary phase becomes narrower. Such results agree with the prediction of Flory lattice theory [29], in which the Flory–Huggins interaction parameter χ controls the solvent quality.

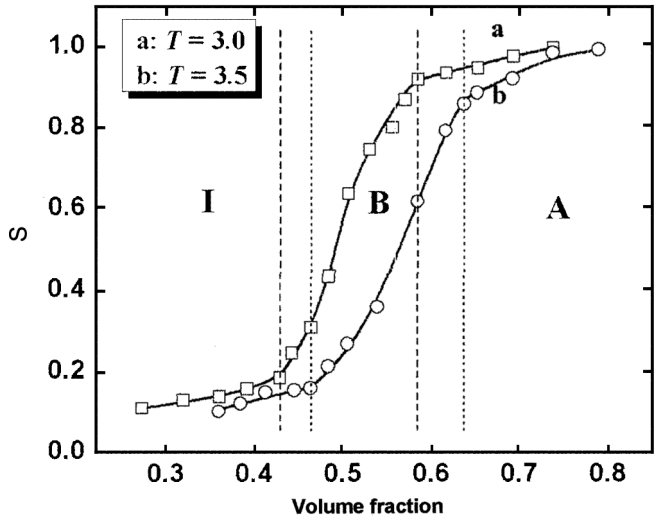

FIGURE 8 Concentration dependence of order parameter at different temperatures *(T)* with $T = 3.0$ (a) and 3.5 (b): I, isotropic phase; B, binary phase; and A, anisotropic phase.

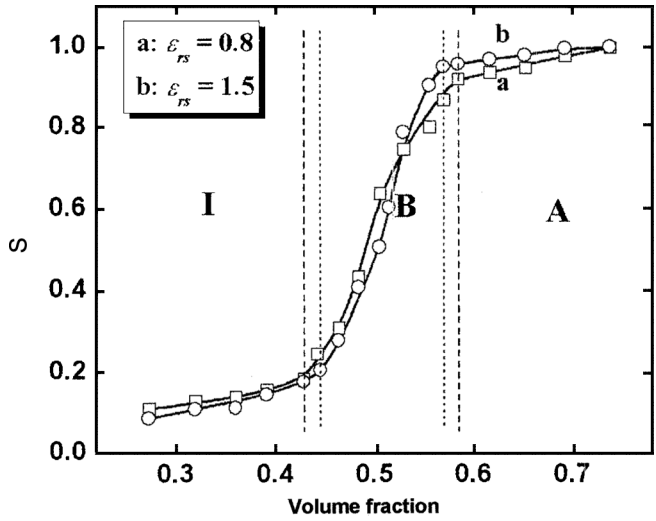

FIGURE 9 Effects of rod–solvent interaction parameter ε_{rs} on the phase behavior for $\varepsilon_{rs} = 0.8$ (a) and 1.5 (b): I, isotropic phase; B, binary phase; and A, anisotropic phase.

Relatively weak solvent-quality dependence and appreciate temperature dependence of transition behavior may indicate that the primary factor for chain alignments in lyotropic LC formation are not rod–solvent interactions, but the excluded-volume effects of rod-like molecules that may have temperature-dependent chain rigidity. Such results agree with the predictions by Onsager [1] and Isihara [30], where they found the excluded volume plays a dominant role in phase separation in dilute solutions of highly asymmetric particles (rods, ellipsoids, or disks). On the other hand, for the lyotropic LC solution, solvent also plays an important role in the phase behavior. Incorporating solvent into the rod-like molecules system can affect the alignment of rod-like molecules and further vary phase property because of the change of rod-like molecule concentration. Meanwhile, the quality of solvent can shift the phase transition in the lyotropic LC system.

Apparent Changes in Chain Rigidity upon Anisotropic Phase Formation

As we mentioned before, the rod-like molecular chain is realized by the bond potential and angle potential. The setting value of angle spring constant k_a can change the molecule rigidity from rigid to flexible conformation. The influences of k_a on the phase diagram and apparent molecular flexibility are specified in Fig. 10. Three cases of k_a with the value of 10,000 (plot i), 5,000 (plot ii), and 2,000 (plot iii) are presented for a rod-like molecule with chain length $L = 9.75$. With decreasing k_a from 10,000 to 2,000, shown in Fig. 10a, the S curve moves to the higher volume fraction, suggesting both IB and BA phase-transition concentrations are increased as k_a is decreased. Simultaneously the binary phase range became narrower.

Shown in Fig. 10b is the apparent molecular flexibility F_m as a function of volume fraction for different k_a. For each plot of F_m, a negligible change on F_m can be found at lower concentrations (in the isotropic phase), and then decreased with increasing volume fraction (in binary and anisotropic phases), suggesting apparent molecule rigidity increased with concentration. We can see that F_m decreases with decreasing k_a at the same volume fraction, as expected.

In the isotropic range, the rod-like molecules departed from each other and exist surrounded by solvent molecules. In this case, the persistence length of the rod-like molecule is independent of concentration (see Fig. 10b), as expected, and is considered to be intrinsic to molecular structure. For our model we obtain the following persistence lengths, l_p: for $k_a = 10{,}000$ $l_p = L/F_{m,i} \approx 48$, for $k_a = 5{,}000$ $l_p \approx 36$, and for $k_a = 2{,}000$ $l_p \approx 22$ (the subscript i in $F_{m,i}$ denotes the isotropic

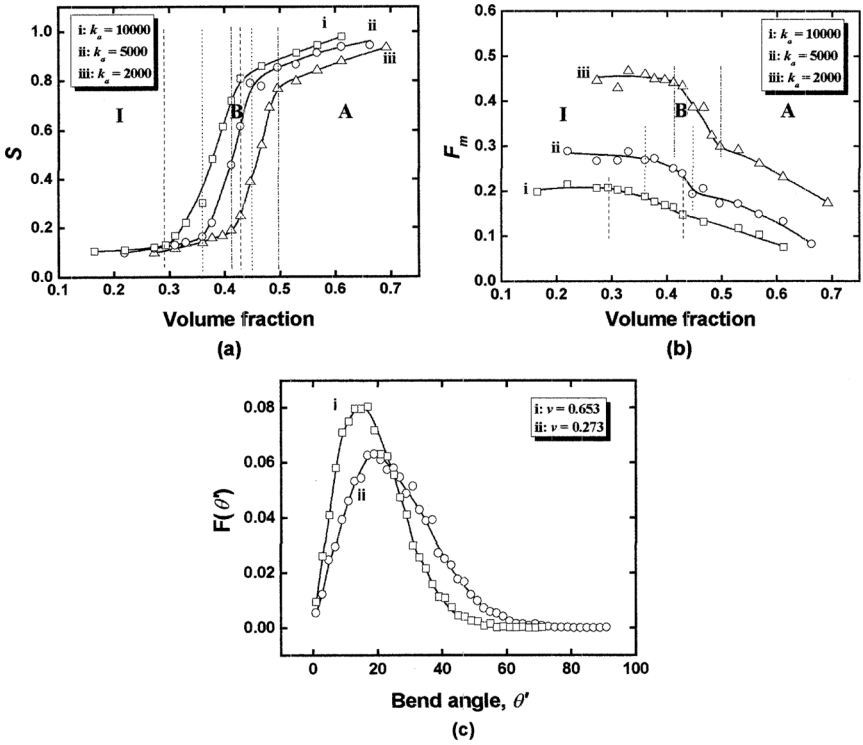

FIGURE 10 Order parameter S (a) and apparent molecular flexibility F_m (b) as a function of concentration for $L = 9.75$ at different k_a values: $k_a = 10{,}000$ (i), $k_a = 5{,}000$ (ii), and $k_a = 2{,}000$ (iii): I, isotropic phase; B, binary phase; and A, anisotropic phase. (c) Typical results of the bending-angle distribution function $F(\theta')$ for $L = 6.75$ and $k_a = 10{,}000$ at different volume fractions: (i) $v = 0.653$ and (ii) $v = 0.273$..

phase). As volume fraction increased, partial rod molecules with less surrounding solvents tend to align because of the exclude volume and attractive interaction between rod pairs, which results in a higher order as shown in Fig. 10a. Meanwhile, such an alignment gives less volume for rod-like molecules to bend, which induces to a smaller F_m. With further increasing volume fraction, more and more rod-like molecules take part into alignment. The system translates from binary phase into anisotropic phase. We can obtain the apparent persistence lengths in the anisotropic phase: for $k_a = 10{,}000$ $L_p \approx 66$, for $k_a = 5{,}000$ $L_p \approx 50$, and for $k_a = 2{,}000$ $L_p \approx 32$. Further decreasing of F_m can be also observed in the anisotropic phase. The decrease of apparent flexibility with increasing volume fraction implies the decrease in bending of

rod-like molecules with molecular alignments. To see more details of the change in molecular bending and alignments with LC formation, we calculate the normalized distribution function, $F(\theta')$, of bending angles in isotropic and anisotropic phases, which is shown in Fig. 10c. Here the bending angle, θ', is defined by the angle between the bond vectors of two ends of a rod-like molecule. At the higher volume fraction (0.653) in the LC phase, the bending-angle distribution is narrower, having a peak at a smaller angle (less bending) compared with the distribution at a lower volume fraction (0.273) in the isotropic phase. This clearly shows the feature of molecular alignments in the LC phase, where the rod-like molecules have less bending and any molecules are not allowed to largely deviate from the average bending angle because the rods are aligning together to form an ordered phase.

Shown in Fig. 11a is the dependence of phase-transition concentrations of IB and BA on the $1/k_a$ for the rod-like molecules with $L = 9.75$. With decreasing $1/k_a$, increasing the apparent molecular rigidity, phase-transition concentrations of both IB and BA move to the lower values. Concomitantly the boundary of binary phase is widened. Extrapolating curves (i) and (ii) to the extreme case of $1/k_a = 0$ (i.e., $k_a = \infty$), shown as dash lines in Fig. 11a, we can obtain the transition concentrations of both IB and BA for the perfect rigid rod. The apparent molecular flexibility F_m as a function of $1/k_a$ is illustrated in Fig. 11b. F_m at phase-transition points of both IB and BA are decreased with decreasing $1/k_a$. The trends of F_m for phase transitions with lower $1/k_a$ are illustrated as dashed lines shown in Fig. 11b.

The dependence of apparent persistence length L_p at phase transitions on molecular chain length L is illustrated for $ka = 10{,}000$ in Fig. 12. L_p doesn't change with L in the isotropic phase, which confirms that L_p in isotropic phase is the intrinsic one, being equal to l_p. In contrast, L_p in the LC phase first decreases with increasing L and then tends to level off, which indicates that the effect of chain alignments on the apparent persistence length is pronounced at shorter chains and very weak for longer chains.

It is meaningful to compare our results with theoretical predictions. Based on the Onsager theory, Khokhlov–Semenov (KS) used the second viral expansion for the solution containing a wormlike polymer with the diameter D [3]. The KS expressions can be written as follows:

$$c_i = \frac{3.34 + 5.97L/l_p + 1.585(L/l_p)^2}{L/l_p(1 + 0.293L/l_p)}, \tag{9}$$

$$c_a = \frac{4.486 + 11.24L/l_p + 17.54(L/l_p)^2}{L/l_p(1 + 2.83L/l_p)}, \tag{10}$$

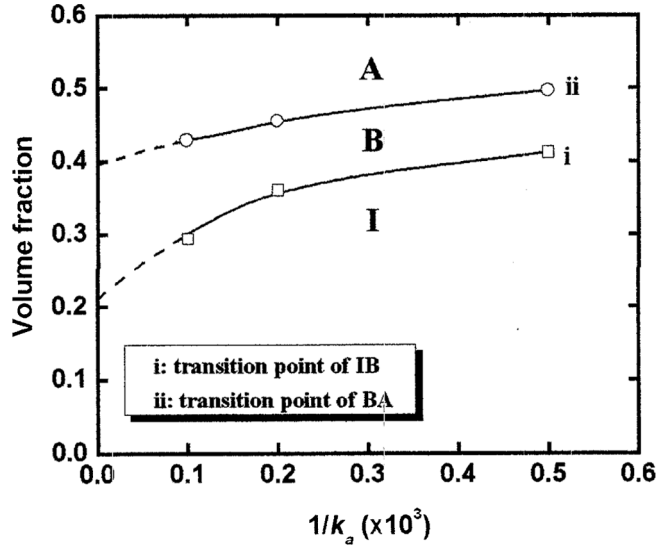

(a)

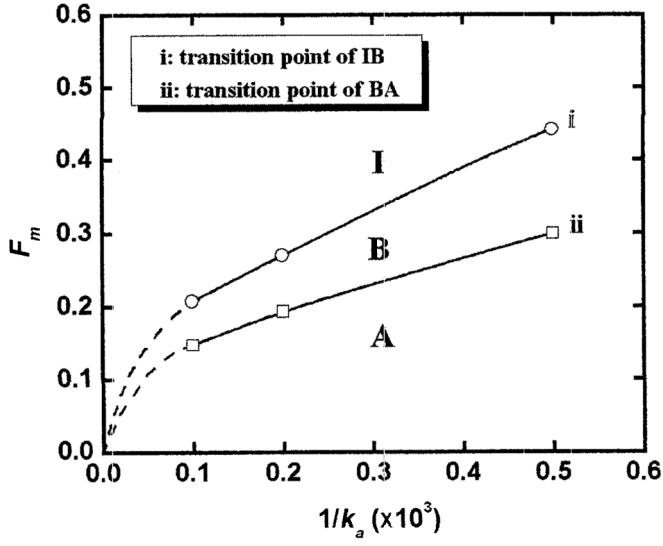

(b)

FIGURE 11 Phase-transition concentrations (a) and apparent molecular flexibility F_m (b) as a function of $1/k_a$ for $L = 9.75$: I, isotropic phase; B, binary phase; and A, anisotropic phase.

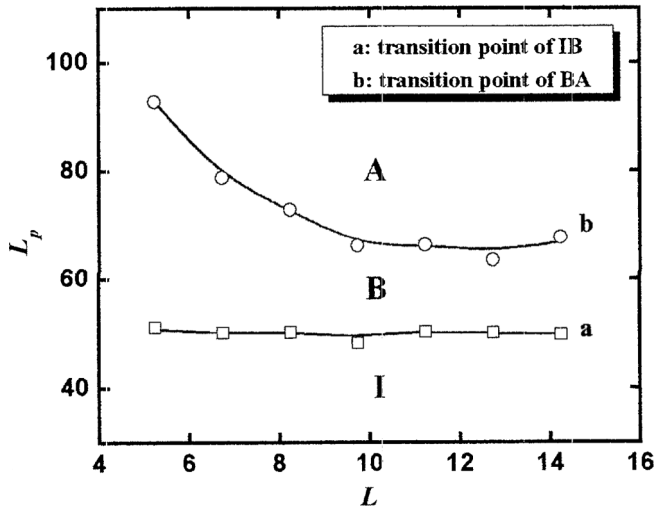

FIGURE 12 Apparent persistence length L_p vs. chain length L at the phase-transiton points of (a) IB and (b) BA for $k_a = 10{,}000$: I, isotropic phase; B, binary phase; and A, anisotropic phase.

$$S = \frac{0.844 + 3.488L/l_p + 0.610(L/l_p)^2}{1 + 5.874L/l_p + (L/l_p)^2}, \tag{11}$$

where subscripts i and a correspond to isotropic and anisotropic phases, respectively. The dimensionless parameter c can be written by [3]

$$c = bc'\frac{l_p}{L} = \frac{\pi}{4}L^2 D\frac{N}{V}\frac{l_p}{L} = \phi\frac{l_p}{D}, \tag{12}$$

where the quantity b is half of the excluded volume between two rod-like molecules; $c' = N/V$ is the number density, V is the system volume, and $\phi = (\pi D^2 L/4)N/V$ is the volume fraction of rod-like molecules:

$$\phi_i = \left(\frac{D}{L}\right)\frac{3.34 + 5.97L/l_p + 1.585(L/l_p)^2}{1 + 0.293L/l_p},$$

$$\phi_a = \left(\frac{D}{L}\right)\frac{4.486 + 11.24L/l_p + 17.54(L/l_p)^2}{1 + 2.83L/l_p}.$$

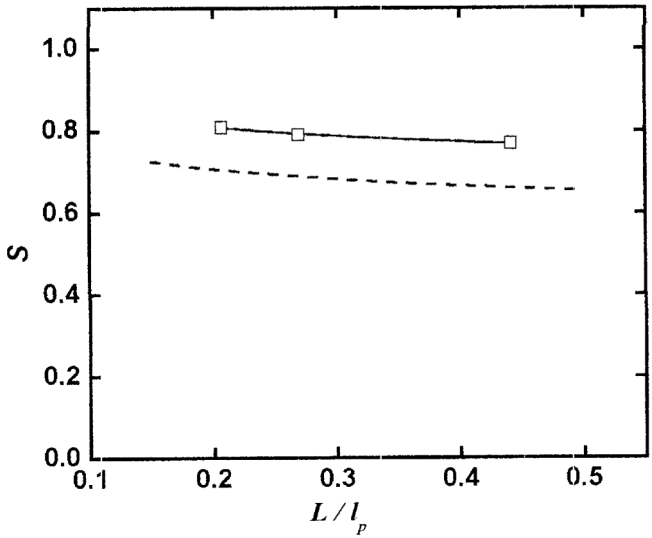

FIGURE 13 Order parameter S at BA phase transition as a function of L/l_p. Open squares: simulation results. Dashed line: Khokhlov–Semenov theory [Eq. (11)].

In the following comparisons, we use the l_p obtained in the isotropic phase as mentioned previously, and for the volume fraction, ϕ, we use the volume fraction obtained here (see section on volume fraction). Shown in Fig. 13 is the order parameter S at BA phase transition as a function of L/l_p. The S value is decreased in our simulation with increasing L/l_p, which coincides with the theoretical prediction of KS shown by a dashed line. Plots of the reduced volume fractions, ϕ_i and ϕ_a, at the phase transitions of IB and BA as a function of L/l_p are presented in Fig. 14. Shown in Fig. 14a are the simulation results at fixed $L = 9.75$ with different l_p values. The simulation results at fixed $l_p = 50$ ($k_a = 10{,}000$) with different L are shown in Fig. 14b compared with the theoretical predictions of Eqs. (9) and (10). The simulation results are qualitatively in line with the theoretical predictions. The deviation between simulation results and theory prediction may partly be due to the difference in volume fraction used. The volume fraction obtained from the simulation is more real, which is slightly different from the theoretically defined one. Such a deviation between simulation and theoretical results was also found by Kolb [24] and Yethiraj and Fynewever [31] for semiflexible molecules in bulk as $L/l_p > 0.1$.

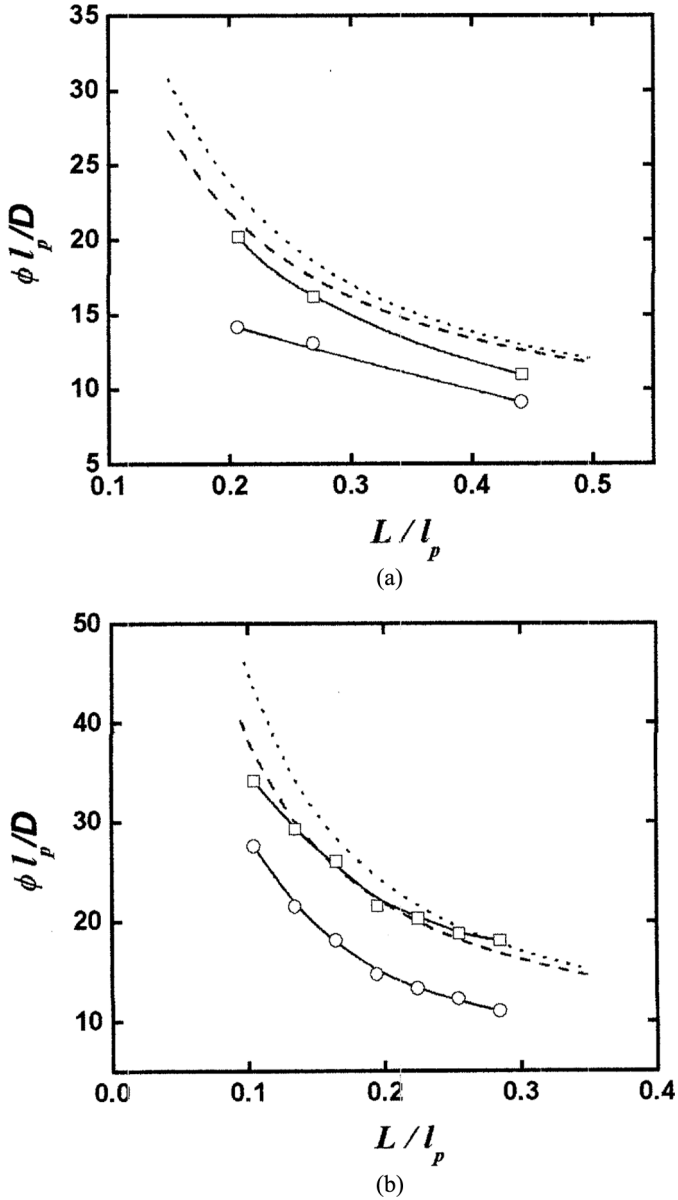

FIGURE 14 Volume fractions at the phase transition of IB and BA as a function of L/l_p. Simulation results: open circles, IB phase transition; open squares: BA phase transition, Khokhlov–Semenov theory; dashed, IB phase transition [Eq. (9)]; dotted, BA phase transition [Eq. (10)]. (a) L/l_p at fixed $L = 9.75$; (b) L/l_p at fixed $l_p = 50$ ($k_a = 10{,}000$).

CONCLUSIONS

Coarse-grain MD simulations are carried out for the lyotropic LC solutions involving semiflexible rod-like molecules. Phase behavior is investigated in terms of order parameter, and MD information is specified. The influences of chain length, chain flexibility, temperature, and rod–solvent interactions are studied. Comparisons with simulation results and theoretical predictions are also carried out. The main conclusions are as follows:

(1) We provide another model for a rod-like molecule, which is realized by harmonic-stretching potential and angle-bending potential. The advantage of such a model is that the rigidity of the molecule can be designed from rigid to flexible conformation.
(2) Phase behavior of lyotropic LC solution is specified by the MD simulation. With increasing the rod-like molecule volume fraction, the solution transits from isotropic to binary phase and then to anisotropic phase. The phase transitions tend to occur at lower concentrations with increasing rod-like chain length or decreasing temperature. Predictions by the simulations on the influences of chain length and solvent quality are in line with the Flory lattice theory for rod-like molecule solution. It confirms that the present coarse-grained model is satisfactory in application for LC solutions of rod-like molecules.
(3) The decrement of chain rigidity increases the incipient concentration of phase transitions, and the apparent persistence length is increased by molecular alignments with LC formations at higher concentrations. The simulation results are qualitatively in good agreements with theoretical predictions by Khokhlov and Semenov.

ACKNOWLEDGMENTS

This work was supported by a Grant-in-Aid for "Academic Frontier" Project for Private Universities; matching fund subsidy from Ministry of Education, Culture, Sports, Science and Technology (MEXT), Japan, 2001–2005 and 2006–2008; and National Natural Science Foundation of China (20574018, 50673026). Support from Program for New Century Excellent Talents in University in China (NCET-04–0410) is also appreciated.

REFERENCES

[1] Onsager, L. (1949). *Ann. N. Y. Acad. Sci.*, *51*, 627.
[2] Flory, P. J. (1956). *Proc. R. Soc. London*, *A234*, 60.

[3] Odijk, T. (1986). *Macromolecules*, *19*, 2313.
[4] Hermans, J. Jr. (1962). *J. Colloid. Sci*., *17*, 638.
[5] Nakajima, A., Hayashi, U., & Ohmori, M. (1968). *Biopolymers*, *6*, 973.
[6] Porter. R. (1974). *Liquid Crystals and Ordered Fluids*, Plenum Press: New York.
[7] Kiss, G. & Porter, R. (1978). *J. Polym. Sci. Polym. Symp*., *65*, 193.
[8] Aharoni, S. M. & Walsh, E. K. (1979). *Macromolecules*, *12*, 271.
[9] Conio, G., Bianchi, E., Ciferri, A., & Tealdi, A. (1981). *Macromolecules*, *14*, 1084.
[10] Ciferri, A. (1991). *Liquid Crystallinity in Polymers*, VCH: New York.
[11] Metropolis, N., Rosenbluth, A. W., Rosenbluth, M. N., Teller, A. H., & Teller, E. (1953). *J. Chem. Phys*., *21*, 1087.
[12] Wood, W. W. & Parker, F. R. (1957). *J. Chem. Phys*., *27*, 720.
[13] Alder, B. J. & Wainwright, T. E. (1957). *J. Chem. Phys*., *27*, 1208.
[14] Stroobants, A., Lekkerkerker, H. N. W., & Frenkel, D. (1987). *Phy. Rev. A*, *36*, 2929; Frenkel, D., Lekkerkerker, H. N. W., & Stroobants, A. (1988). *Nature*, *332*, 822.
[15] Hess, S., Frenkel, D., & Allen, M. P. (1991). *Mol. Phys*., *74*, 765; Camp, P. J. & Allen, M. P. (1997). *J. Chem. Phys*., *106*, 6681; Allen, M. P. (1999). *Computer Physics Communications*, *121–122*, 219.
[16] Gay, J. G. & Berne, B. J. (1981). *J. Chem. Phys*., *74*, 3316.
[17] Palke, W. E., Emsley, J. W., & Tildesley, D. J. (1994). *Mol. Phys*., *82*, 177.
[18] Dijkstra, M. & Frenkel, D. (1995). *Phy. Rev. E*, *51*, 5891.
[19] Baumgartner, A. (1986). *J. Chem. Phys*., *84*, 1905.
[20] Kolinsky, A., Skolnick, J., & Yaris, R. (1986). *Macromolecules*, *19*, 2560.
[21] Tian, P., Bedreov, D., & Smith, G. D. (2001). *J. Chem. Phys*., *115*, 9055.
[22] Paolini, G. V., Ciccotti, G., & Ferrario, M. (1993). *Mol. Phys*., *80*, 297.
[23] Affouard, F., Kroger, M., & Hess, S. (1996). *Phys. Rev. E*, *54*, 5178.
[24] Darinskii, A. A., Zarembo, A., Balabaev, N. K., Neelov, I. M., & Sundholm, F. (2003). *Phys. Chem. Chem. Phys*., *5*, 2410; Darinskii, A. A., Neelov, I. M., Zarembo, A., Balabaev, N. K., Sundholm, F., & Binder, K. (2003). *Macromol. Symp*., *191*, 191.
[25] Sakurai, Y. & Ono, I. (2000). *Mol. Cryst. Liq. Cryst*., *346*, 137.
[26] http://octa.jp. OCTA homepage; version: COGNAC4.0.
[27] Berendsen, H. J. C., Postma, J. P. M., van Gunsteren, W. F., Dinola, A., & Haak, J. R. (1984). *J. Chem. Phys*., *81*, 3684.
[28] Baranyai, A. & Cummins, P. T. (1995). *Phys. Rev. E*, *52*, 2198.
[29] Flory, P. J. (1984). *Advances in Polymer Science*, *59*, 1.
[30] Isihara, A. (1951). *J. Chem. Phys*., *19*, 1142.
[31] Yethiraj, A. & Fynewever, H. (1998). *Mol. Phys*., *93*, 693.